Vacuolar Phosphate Transporters Contribute to Systemic Phosphate Homeostasis Vital for Reproductive Development in Arabidopsis[1][OPEN]

Mingda Luan,[a,b] Fugeng Zhao,[a] Xingbao Han,[a] Guangfang Sun,[a] Yang Yang,[a] Jinlong Liu,[c] Jisen Shi,[d] Aigen Fu,[b] Wenzhi Lan,[a,2] and Sheng Luan[e,3]

[a]Nanjing University-Nanjing Forestry University Joint Institute for Plant Molecular Biology, School of Life Sciences, Nanjing University, Nanjing 210093, People's Republic of China
[b]The Key Laboratory of Western Resources Biology and Biological Technology, College of Life Sciences, Northwest University, Xi'an 710069, People's Republic of China
[c]College of Animal Science & Technology, Northwest A&F University, Yangling, Shanxi 712100, China
[d]Nanjing University-Nanjing Forestry University Joint Institute for Plant Molecular Biology, Key Laboratory of Forest Genetics and Biotechnology, Nanjing Forestry University, Nanjing 210037, People's Republic of China
[e]Department of Plant and Microbial Biology, University of California, Berkeley, California 94720

ORCID IDs: 0000-0001-8772-6733 (M.L.); 0000-0002-4906-9856 (F.Z.); 0000-0002-3376-9233 (J.S.); 0000-0002-9207-7915 (W.L.); 0000-0002-8375-8276 (S.L.).

Vacuolar storage of phosphate (Pi) is essential for Pi homeostasis in plants. Recent studies have identified a family of vacuolar Pi transporters, VPTs (PHT5s), responsible for vacuolar sequestration of Pi. We report here that both VPT1 and VPT3 contribute to cytosol-to-vacuole Pi partitioning. Although VPT1 plays a predominant role, VPT3 is particularly important when VPT1 is absent. Our data suggested that the *vpt1 vpt3* double mutant was more defective in Pi homeostasis than the *vpt1* single mutant, as indicated by Pi accumulation capacity, vacuolar Pi influx, subcellular Pi allocation, and plant adaptability to changing Pi status. The remaining member of the VPT family, VPT2 (PHT5;2), did not appear to contribute to Pi homeostasis in such assays. Particularly interesting is the finding that the *vpt1 vpt3* double mutant was impaired in reproductive development with shortened siliques and impaired seed set under sufficient Pi, and this phenotype was not found in the *vpt1 vpt2* and *vpt2 vpt3* double mutants. Measurements of Pi contents revealed Pi over-accumulation in the floral organs of *vpt1 vpt3* as compared with the wild type. Further analysis identified excess Pi in the pistil as inhibitory to pollen tube growth, and thus seed yield, in the mutant plants. Reducing the Pi levels in culture medium or mutation of PHO1, a Pi transport protein responsible for root-shoot transport, restored the seed set of *vpt1 vpt3*. Thus, VPTs, through their function in vacuolar Pi sequestration, control the fine-tuning of systemic Pi allocation, which is particularly important for reproductive development.

Phosphorus (P), an essential macronutrient for plant growth, plays vital roles in most metabolic processes in plants. Phosphate (Pi) is the major available form of P that can be used by plants, but the concentration of Pi is extremely low (typically less than 10 μM) in the soil and often supplemented by fertilizers for sustainable crop production (Withers et al., 2014). However, phosphorus rock, a major source of Pi fertilizer, is a nonrenewable and unevenly distributed natural resource on earth (Vance et al., 2003; Van Kauwenbergh et al., 2013). Thus, improving P nutrient use efficiency becomes an urgent demand for sustainable agriculture. This requires understanding of the genetic network that controls Pi transport and homeostasis in plants. Along this line, research efforts have been focused on the identification of transporters involved in Pi uptake, translocation, and storage (Gu et al., 2016; Młodzińska and Zboińska, 2016; Luan et al., 2017). *PHOSPHATE TRANSPORTER 1* (*PHT1*) family members are the primary transporters for Pi uptake (Misson et al., 2004; Shin et al., 2004; Ai et al., 2009; Jia et al., 2011; Wang et al., 2014). In Arabidopsis (*Arabidopsis thaliana*), nine *PHT1* members are induced by low Pi, and the Pi uptake efficiency of the *pht1;1 pht1;4* double mutant is reduced by more than 60% compared with the wild type (Shin et al., 2004). Under Pi sufficient conditions,

[1]This work was supported by the National Natural Science Foundation of China (NSFC) (grant no. 31770267 to W.L. and grant no. 31770266 to F.Z.) and the National Science Foundation (to S.L.).

[2]Senior author.

[3]Author for contact: sluan@berkeley.edu.

The author responsible for distribution of materials integral to the findings presented in this article in accordance with the policy described in the Instructions for Authors (www.plantphysiol.org) is: Sheng Luan (sluan@berkeley.edu).

M.L., W.L., and S.L. designed the research, analyzed the data, and wrote the article; M.L., F.Z., X.H., G.S., J.L. and Y.Y. conducted the experiments and analyzed the results; J.S. and A.F. provided some facility and reagents for the research.

[OPEN]Articles can be viewed without a subscription.

www.plantphysiol.org/cgi/doi/10.1104/pp.18.01424

PHT1 proteins are degraded through a PHOSPHATE 2 (PHO2)–mediated ubiquitin-dependent pathway (Huang et al., 2013). Loss-of-function of PHO2 results in higher levels of PHT1 proteins, which causes over-accumulation of Pi under Pi-sufficient conditions (Huang et al., 2013). Another type of transporter is represented by PHOSPHATE 1 (PHO1), an SPX [Syg1 (Suppressor of Yeast gpa1), Pho81 (yeast Phosphatase 81), and Xpr1 (human Xeno-tropic and Polytropic Retrovirus receptor 1)] domain-containing protein, and the SPX domain has recently been defined as a "Pi sensing" domain (Wild et al., 2016). PHO1 is localized to the trans-Golgi network and is mainly expressed in pericycle tissues (Arpat et al., 2012), in which it facilitates Pi loading into xylem for translocation from roots to shoots (Hamburger et al., 2002). Lack of PHO1 leads to low Pi stress in the upper parts (leaves, stem, and flowers) of plants (Poirier et al., 1991). For subcellular Pi homeostasis, Pi sequestration into the vacuole plays a key role in temporary storage of cellular Pi. Recent studies demonstrate that VACUOLAR PHOSPHATE TRANSPORTER 1 (VPT1 or PHT5;1) contributes to Pi sequestration in the vacuole (Liu et al., 2015, 2016b). VPT1, also an SPX domain-containing protein, is localized at the tonoplast, and loss of its function results in low vacuolar Pi content and impairs plant adaptation to changing Pi status in the environment. All of the phosphate transporters identified so far play important roles in Pi homeostasis, which is critical for plant growth.

In addition to supporting vegetative growth, Pi is also essential for reproduction in plants. In agriculture, Pi deficiency in the soil often reduces seed-setting, leading to lower crop yield (Marschner, 1986; Mu et al., 2008). Several studies using the Arabidopsis model have linked Pi homeostasis to reproductive development. For example, loss of PHO1 inhibits root-shoot Pi translocation and causes late flowering and low seed yield as a result of low Pi availability for reproductive development (Poirier et al., 1991). Overexpression of miR399, a negative regulator of At*PHO2*, or loss-of-function of AtPHO2 induces early flowering, which might be related to over-accumulation of Pi (Kim et al., 2011). In rice (*Oryza sativa*), loss of OsPHO2 or its interaction protein OsGIGANTEA mimics the Pi starvation response, which may contribute to late flowering (Li et al., 2017). Despite these examples connecting Pi status to reproductive development, much needs to be done on the mechanisms linking Pi homeostasis to reproduction.

In this study, we conducted genetic analysis of three *VPT* family members, including *VPT1* (AT1G63010), *VPT2 (*AT4G11810), and *VPT3* (AT4G22990), following the nomenclature in Arabidopsis (Liu et al., 2015). We found that VPT3 contributed to vacuolar Pi transport activity, especially in the *vpt1* mutant background. Loss-of-function of VPT2 did not affect Pi homeostasis in Arabidopsis. Importantly, we uncovered a strong association of VPT1 and VPT3 function with reproductive development. Our genetic data suggested loss of both VPT1 and VPT3 leads to impaired seed set under sufficient Pi conditions. We further demonstrated that reduced Pi sequestration into leaf vacuoles in *vpt1 vpt3* double mutant increased Pi allocation into the floral organs, leading to over-accumulation of Pi in the pistil. High levels of Pi in pistil tissue inhibits pollen tube growth and thereby reduces seed set. Thus, this study has revealed a previously unanticipated role of vacuolar sequestration in maintaining systemic Pi allocation critical for plant reproduction.

RESULTS

VPT3 Contributes to Vacuolar Pi Sequestration in the *vpt1* Mutant Background

Previous studies identified three *SPX-MFS* genes named *VPT1, VPT2*, and *VPT3*, also termed *PHT5;1, PHT5;2*, and *PHT5;3* (Liu et al., 2016b). The expression patterns of *VPT* family members appeared to be overlapping, and all of them are universally expressed in most plant tissues including roots, leaves, and flowers. In leaves, *VPT2* was preferentially expressed in guard cells (Supplemental Fig. S1). It has been validated that all of them are localized to the tonoplast (Supplemental Fig. S2; Liu et al., 2015, 2016b). Among the three members, VPT1 (PHT5;1) is the major contributor to Pi sequestration in the vacuole, because the *vpt1* single mutant shows an obvious defect in Pi homeostasis. In this study, we further investigated the function of other VPTs by genetic analysis. We obtained T-DNA lines for each *VPT* gene, including *vpt1-1* (*pht5;1-2*), *vpt1-2* (*pht5;1-3*), *vpt2* (*pht5;2*), and *vpt3* (*pht5;3*; Supplemental Fig. S3A). The *vpt1* single mutants showed growth retardation and accumulate less Pi as compared with the wild type and other single mutants (Supplemental Fig. S3,B–D). The *vpt2* and *vpt3* single mutants did not show a significant difference from the wild type. To further clarify the function of VPT2 and VPT3, we generated various double mutants and a triple mutant including *vpt1 vpt2* (*vpt1-1 vpt2*), *vpt1 vpt3* (*vpt1-1 vpt3* and *vpt1-2 vpt3*), *vpt2 vpt3* (*vpt2 vpt3*), and *vpt1 vpt2 vpt3* (*vpt1-1 vpt2 vpt3*; Fig. 1A). Pi contents in all the mutants lacking VPT1 (*vpt1*, *vpt1 vpt2*, *vpt1 vpt3*, and *vpt1 vpt2 vpt3*) were dramatically decreased when compared with wild type, whereas Pi content was not altered in the *vpt2 vpt3* double mutant (Fig. 1, A and B). The Pi contents of *vpt1* and *vpt1 vpt2* were comparable. Although all mutants lacking VPT1 (including *vpt1*, *vpt1 vpt2*, *vpt1 vpt3*, and *vpt1 vpt2 vpt3*) were comparable in fresh weight and root length (Supplemental Fig. S4), *vpt1 vpt3* and *vpt1 vpt2 vpt3* had lower Pi contents than the *vpt1* single mutant (Fig. 1, A and B). The low-Pi content phenotype of the *vpt1 vpt3* double mutant was complemented by transforming the double mutant with a genomic fragment containing either *VPT1* (COMVPT1) or *VPT3* (COMVPT3; Supplemental Fig. S5). The Pi content of *vpt1 vpt3* COMVPT1 was comparable with the *vpt3* single mutant and wild type,

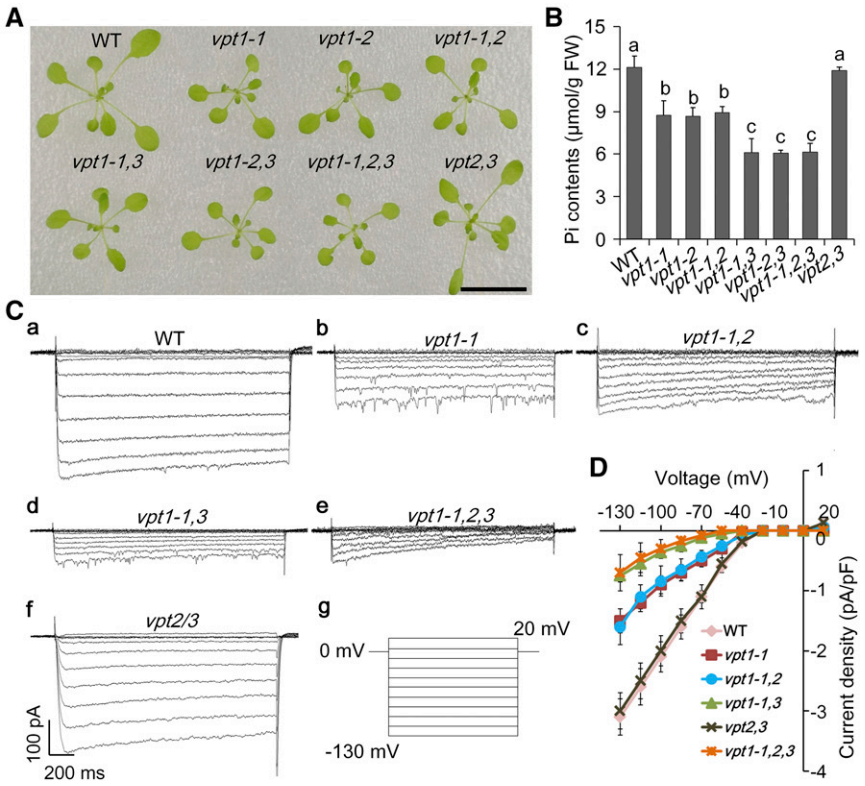

Figure 1. vpt3 contributes to vacuolar Pi sequestration in *vpt1*. A, Growth phenotype of 16-d-old seedlings (*vpt1-1 vpt2*, *vpt1-1 vpt3*, *vpt1-2 vpt3*, *vpt1-1 vpt2 vpt3*, *vpt2 vpt3* are abbreviated as *vpt1-1,2*; *vpt1-1,3*; *vpt1-2,3*; *vpt1-1,2,3*; *vpt2,3* in all the figures of this study) cultured in hydroponic solution with 130 μM Pi. Bar = 2 cm. B, Seedlings in (A) were gathered for Pi content measurements. Different letters above each bar indicate statistically significant differences ($P < 0.05$, Tukey's honestly significant difference [HSD] test). Error bars indicate ± SD; $n = 3$ technical replicates × 4 biological replicates. FW, fresh weight. C, Whole-vacuole Pi currents were reduced in the vacuoles from *vpt1* mutants. Representative Pi current traces recorded in whole-vacuole configuration from wild type (WT) (a), *vpt1* single mutant (b), three double mutants (*vpt1 vpt2*, *vpt1 vpt3*, *vpt2 vpt3*) (c, d, f), and one triple mutant (*vpt1 vpt2 vpt3*) (e). With a holding potential of 0 mV, currents were evoked in −15 mV steps in the voltage range from +20 to −130 mV (g). Steady-state currents were determined by averaging the first 50 ms of each current trace for inward currents. D, The current-voltage curves were derived from whole-vacuole Pi currents as in (C). Results were are as means ± SD from three independent experiments; $n = 9 \sim 12$.

whereas *vpt1 vpt3* COMVPT3 was similar to the *vpt1* single mutant (Supplemental Fig. S5E). Therefore, both VPT1 and VPT3, but not VPT2, contribute to Pi accumulation in plant tissues.

The vacuole contains the major pool of stored Pi in the plant cell (Pratt et al., 2009), and disruption of vacuole-stored Pi would significantly affect Pi accumulation in plant tissues. All VPT family members are localized at the tonoplast and likely contribute to Pi sequestration into the vacuole (Liu et al., 2015, 2016b). Therefore, we assumed that the different capacities for Pi accumulation in the various genotypes are related to vacuolar Pi sequestration. We used patch-clamp assays to examine vacuolar Pi influx in various double mutants and the triple mutant lacking VPT1, 2, and 3 (Fig. 1C). We isolated intact vacuoles from mesophyll cells of wild-type and mutant plants, and clamped them between +20 and −130 mV with 15-mV decrements. Large time-dependent Pi influx currents were recorded in the wild-type vacuoles at negative test voltages, and under the same experimental conditions, the Pi influx currents recorded from *vpt1* mutant vacuoles were much smaller as compared with wild type (Fig. 1, C and D), consistent with results we reported earlier (Liu et al., 2015). The current density in *vpt1 vpt3* was reduced even further to the level equivalent to nearly 20% of the wild-type current at −130 mV. In contrast, the current density in the *vpt1 vpt2* double mutant was comparable that of the *vpt1* single mutant, at about 35% of the wild-type level. Pi influx currents from the *vpt1 vpt2 vpt3* triple mutant were similar to that from the *vpt1 vpt3* double mutant (Fig. 1D). However, the currents recorded from the *vpt2 vpt3* double mutant did not differ from the wild type.

These electrophysiological results matched the Pi content measurements, indicating that VPT3 is another contributor of vacuolar Pi sequestration. However, VPT3 appeared to play such a role only in the *vpt1* mutant background. One possible explanation for this observation is a compensation effect between the two genes (Shin et al., 2004; Wudick et al., 2018), i.e.

expression of *VPT3* is up-regulated when *VPT1* is disrupted. To test this hypothesis, we used the GUS reporter lines to measure the expression patterns of *VPT1* and *VPT3*. Through genetic crosses, we introduced a p*VPT3-GUS* reporter into the *vpt1* mutant and p*VPT1-GUS* into the *vpt3* mutant. The GUS assays showed that p*VPT3-GUS* was significantly up-regulated in *vpt1*, whereas the expression of *VPT1* was not altered in *vpt3* (Supplemental Fig. S6,A and B). Meanwhile, we conducted reverse transcription quantitative PCR (RT-qPCR) assays to measure the mRNA levels of *VPT1* and *VPT3* in the wild-type and mutant backgrounds, and the results were consistent with the data from the GUS assays. In the *vpt1* mutant, the transcript level of *VPT3* was up-regulated more than 5-fold as compared with its expression level in the wild type, whereas loss of *VPT3* did not affect the level of *VPT1* mRNA (Supplemental Figure S6C). Therefore, up-regulation of *VPT3* could partially compensate VPT1 function in the *vpt1* mutant. This is consistent with the finding that overexpression of *VPT3* enhances Pi accumulation in Arabidopsis (Liu et al., 2016b).

Loss of VPTs Induces Hypersensitivity to Pi Deficiency in Arabidopsis

When confronted with Pi-deficient conditions, the stored cellular Pi will be released to meet the physiological demand of the plants. The vacuole has been shown to be the most important Pi storage pool in plant cells (Pratt et al., 2009). VPTs are vacuolar Pi influx transporters, and loss-of-function of these transporters would severely reduce Pi storage capacity. To further explore the function of VPT genes in plant adaptation to Pi-deficiency, we conducted phenotypic assays on plants that were exposed to Pi-deficient conditions. Seedlings (5 d old) of various genotypes germinated on 1/2 Murashige and Skoog (MS) plates were transferred to a hydroponic culture solution containing 5 μM Pi for 5 d for low-Pi pretreatment. Then the seedlings were transferred to Pi-deficient (0.1 μM) solution and grown for 9 d. Seedlings lacking VPT1 showed stunted growth (Fig. 2A). The *vpt1* mutants also accumulated more anthocyanins than wild type and the *vpt2 vpt3* double mutant. The mutant plants lacking both VPT1 and VPT3, including the *vpt1 vpt3* double mutant and the *vpt1 vpt2 vpt3* triple mutant, were most affected, showing the highest levels of anthocyanins and the lowest fresh weight (Fig. 2, B and C). As acid phosphatase (APase) activity has been shown to be up-regulated when Pi is limited (Wang et al., 2011), we measured root-associated APase activity as an indicator of response to Pi deficiency. As Figure. 2D shows, *vpt1 vpt3* mutants displayed the highest APase activity among the various genotypes, whereas APase activities of the *vpt1* single mutant and the *vpt1 vpt2* double mutant were lower than that of *vpt1 vpt3* but

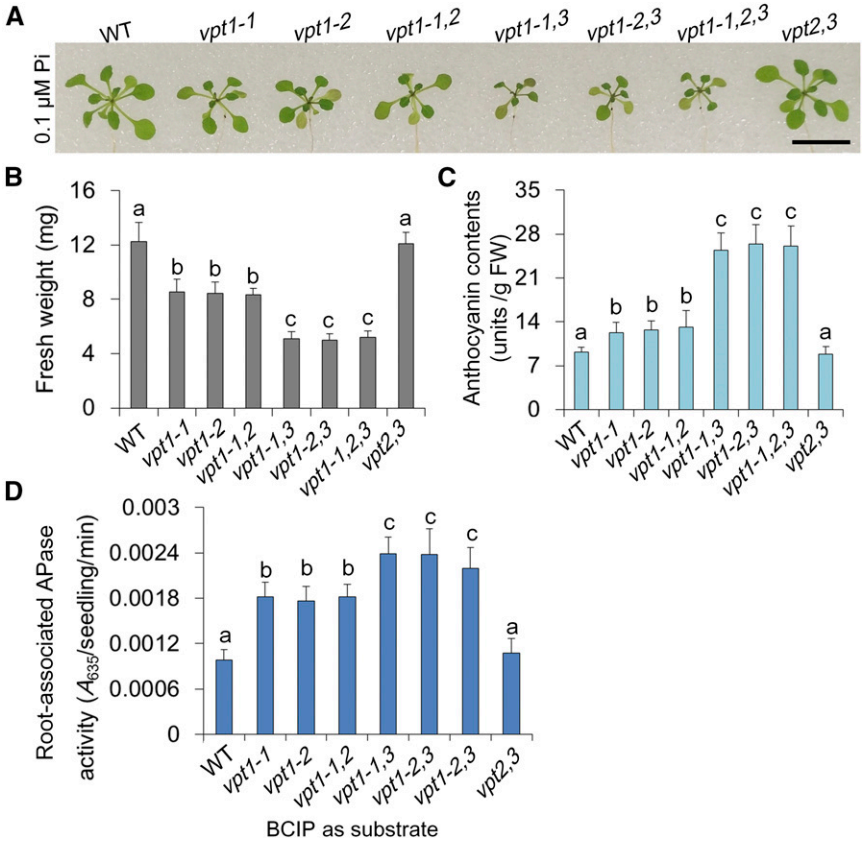

Figure 2. The *vpt1 vpt3* double mutants are hypersensitive to Pi-deficient condition. A, Photographs of the wild-type and various *vpt* mutant plants under Pi-deficient conditions (0.1 μM). Seeds were geminated on 1/2 MS agar medium, and 5-d-old plants were transferred to 5 μM-Pi hydroponic solutions for 5 d. The plants were then transferred to solutions containing 0.1 μM Pi and cultured for another 9 d. WT, wild type. Bars = 1 cm. B, Fresh weight of plants as in (A). C, The anthocyanin contents of various plants grown in 0.1 μM Pi. D, Root-associated APase activities of various plants under Pi-deficient conditions (0.1 μM). Root-associated phosphatase activity was measured as absorption units at 635 nm (A_{635}). In B to D, different letters indicate significant differences among various plant lines. ($P < 0.01$, Tukey's HSD test). Data are means ± SD; $n = 3$ technical replicates × 4 biological replicates.

higher than that of the wild type. Root-associated APase activity of *vpt2 vpt3* was comparable with that of wild type. These results are consistent with the notion that Pi accumulation capacities and vacuolar Pi storage are critical for plants to adapt to Pi limitation.

VPT1 and VPT3 Play a Role in Protection from Pi Toxicity under Changing Pi Status

The vacuole is the major site of Pi storage in plant cells, and our data suggested that VPT1 and VPT3 contribute to vacuolar Pi sequestration, in which manner they could protect plants from Pi toxicity, especially when plants are confronted with robustly elevated Pi in the environment. This kind of protection mechanism should be critical for plant growth under changing Pi status in the soil. Therefore, we examined how well various *vpt* mutants adapted to Pi fluctuations in the culture medium. Seedlings (5 d old) of different genotypes displaying similar growth on half-strength MS medium were transferred to hydroponic solution with 5 μM Pi and cultured for 5 d for low-Pi pretreatment. Then the seedlings were transferred to hydroponic solutions with either 10 μM Pi (low Pi condition) or 300 μM Pi (high Pi condition). On d 8 after transfer, all plants grew similarly under low Pi, but the mutant plants lacking VPT1 were stunted (smaller rosette and shorter roots) in 300 μM Pi as compared with the wild type (Fig. 3, A and B). The fresh weight of *vpt1* and *vpt1 vpt2* were comparable, but *vpt1 vpt3* mutant plants had lower fresh weight and shorter roots than *vpt1* single or *vpt1 vpt2* double mutants, indicating that *vpt1 vpt3* mutant plants were more sensitive to high Pi toxicity following Pi deficiency. The *vpt2 vpt3* double mutant showed no difference from wild type in all conditions. The phenotypes of *vpt1 vpt3* and *vpt1 vpt2 vpt3* were similarly stunted under various Pi conditions (Fig. 3B). Thus, VPT1 and VPT3, but not VPT2, contributed to protection from Pi toxicity under changing Pi status in the environment.

We further examined the consequence of the absence of VPT1 and VPT3 when plants over-accumulate Pi in the *pho2-1* mutant background. Because PHO2 plays a vital role in down-regulating Pi uptake when sufficient Pi is present in the environment, loss of PHO2 leads to hyper-accumulation of Pi in the mutant plants (Aung et al., 2006). We generated various double and triple mutants, including *vpt1-1 pho2-1*, *vpt3 pho2-1*, and *vpt1-1 vpt3 pho2-1*. During phenotyping, we found that *pho2* and *vpt3 pho2* grew better than wild type under low Pi conditions (10 μM), and the Pi contents in these mutants were significantly higher than that in wild-type seedlings (Fig. 4), consistent with the notion that the *pho2* mutant has enhanced Pi uptake capacity (Aung et al., 2006). However, the *vpt1 pho2* double mutant showed stunted growth compared with the wild type (Fig. 4A). This suggests that lack of VPT1 disrupts the capacity of the vacuole to buffer high levels of cellular Pi in *pho2* mutant. These data reinforce the idea that the vacuole is the major Pi pool for buffering cellular Pi (Mimura, 1999; Pratt et al., 2009). Consistent with this idea, the *vpt1 vpt3 pho2* triple mutant showed more severe growth retardation than *vpt1 pho2* (Fig. 4, A and B), indicating loss of VPT3 function further impairs Pi homeostasis. Under the same condition (10 μM Pi), *vpt1*, *vpt3*, and *vpt1 vpt3* showed no phenotypic difference from the wild type, as measured by fresh weight

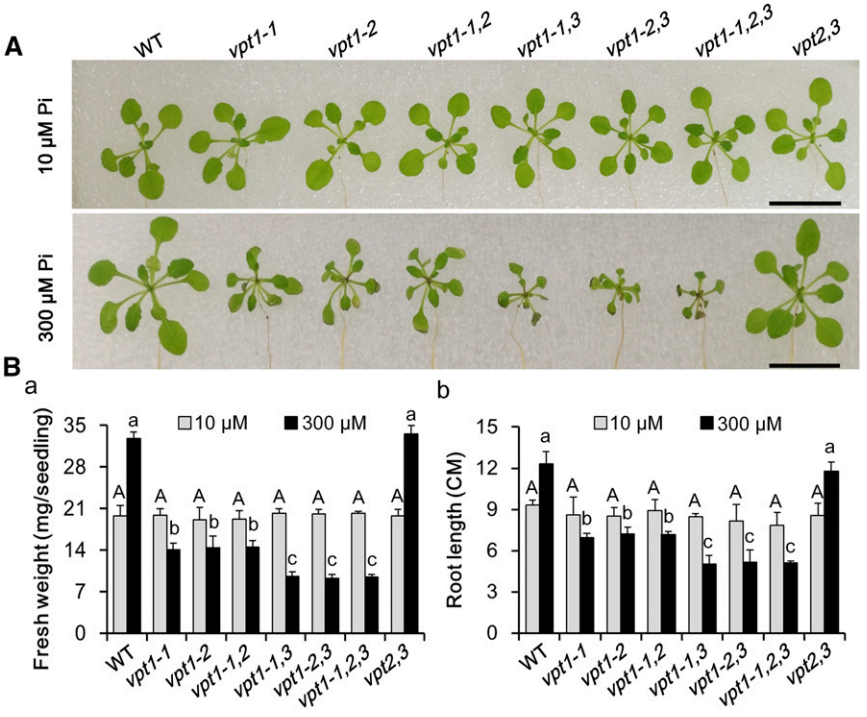

Figure 3. *vpt1* mutants are less adaptable to Pi toxicity under changing Pi status. A, Phenotypes of *vpt* mutants in culture solution with various Pi concentrations. Seeds were germinated on 1/2 MS agar medium, and 5-d-old plants were transferred to 5 μM Pi hydroponic solutions for 5 d. The plants were then transferred to culture solutions containing either 10 μM or 300 μM Pi and cultured for another 8 d. WT, wild type. Bars = 2 cm. B, Fresh weight (a) and root length (b) of seedlings as in (A). Different lowercase letters above each bar represent statistically significant differences among genotypes under 300 μM Pi ($P < 0.01$, Tukey's HSD test). The uppercase letter "A" indicates "no significant difference" under 10 μM Pi. Data are mean ± SD; $n = 3$ technical replicates × 4 biological replicates.

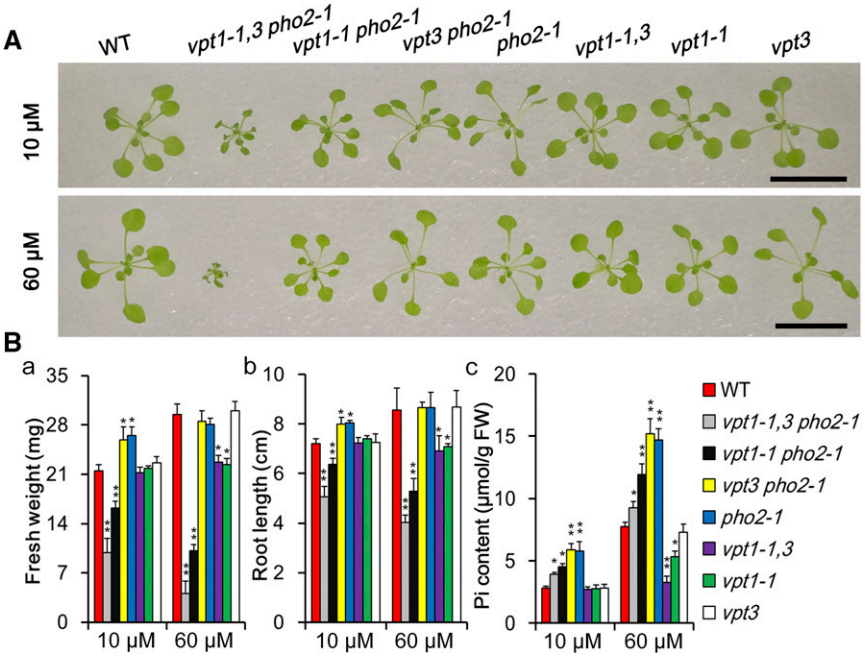

Figure 4. Disruption of VPT1 and VPT3 exacerbates Pi hypersensitivity in the *pho2* mutant. A, Phenotypes of 16-d-old seedlings cultured in hydroponic solution with 10 μM or 60 μM Pi. WT, wild type. Bars = 2 cm. *vpt1-1 vpt3 pho2-1* is abbreviated as *vpt1-1,3 pho2-1*. B, (a) Fresh weight (FW), (b) root length, and (c) Pi contents were measured from seedlings in (A). Data are mean ± SD; $n = 3$ technical replicates × 3 biological replicates. *Significant difference as compared to wild type. Tukey's HSD test, $*P < 0.05$, $**P < 0.01$.

and root length (Fig. 4B). When Pi concentration in the culture solution was adjusted to 60 μM, the *vpt1 vpt3 pho2* triple mutant was very small and severely stunted, but the *vpt1 pho2* double mutant showed less sensitivity to this Pi concentration (Fig. 4, A and B). Therefore, VPT1 and VPT3 are essential for protection from Pi toxicity in Arabidopsis, and these data also support the conclusion that VPT3 contributes to cellular Pi homeostasis in plants when VPT1 is disrupted.

VPT1 and VPT3 Are Essential for Subcellular Pi Allocation

Disruption of vacuolar Pi accumulation should lead to changes in subcellular Pi distribution with more Pi retained in the cytosol. We thus examined subcellular Pi distribution in *vpt* mutants and the wild type using a genetically encoded Pi sensor (cpFLIPPi-5.3m) that monitors Pi concentration in the cytosol (Mukherjee et al., 2015). After crossing the *vpt* mutants with the transgenic sensor lines, we measured the cytosolic Pi concentrations in wild type and the mutants through calculating the fluorescence resonance energy transfer/cyan fluorescent protein (FRET/CFP) fluorescence ratio (Fig. 5A, Supplemental Fig. S7). The *vpt1* single mutant, but not *vpt3* single mutant, contained more Pi in the cytosol than the wild type (Fig. 5, A and B). The cytosolic Pi level in the *vpt1 vpt3* double mutant was the highest (Fig. 5B). However, disruption of VPT2 did not appear to affect the cytosolic Pi level (Fig. 5). These observations suggest that VPT1 is the primary transporter that contributes to cytosol-to-vacuole Pi transport and VPT3 further contributes to intracellular Pi homeostasis, consistent with the earlier results from the electrophysiological analysis (Fig. 1, C and D).

Altered cytosol-to-vacuole Pi transport may affect the expression of the *PSI* (*Phosphate Starvation Induced*) genes, because the expression of these genes depends on cytosolic Pi status. We examined the expression patterns of several *PSI* genes, including *PHT1;1*, *PHT1;4*, *RNS1* (*RNASE 1*), *miR399b*, and *IPS* (*INDUCED BY PHOSPHATE STARVATION 1*) in the wild type and *vpt* mutants by RT-qPCR analysis. The data (Supplemental Fig. S8A) indicated that *PSI* genes were all down-regulated in the *vpt1* single mutant compared with the expression level in the wild-type seedlings, similar to the results reported earlier (Liu et al., 2015, 2016b). Moreover, expression levels of these genes were more severely reduced in the mutants lacking both VPT1 and VPT3 (including *vpt1 vpt3* and *vpt1 vpt2 vpt3*) than in the *vpt1* single mutant (Supplemental Fig. S8A), supporting the idea that Pi homeostasis is more defective in *vpt1 vpt3* mutants. We speculated that loss-of-function of VPTs not only reduces vacuolar Pi sequestration but may also exert a negative effect on Pi uptake due to reduced expression of *PSI* genes, including those encoding the PHT1-type Pi transporters. For instance, when more Pi accumulated in the cytosol in the *vpt1 vpt3* mutants, *PHT1;1* and *PHT1;4*, two genes that contribute to Pi uptake in Arabidopsis, were significantly down-regulated in the *vpt1 vpt3* mutants (Supplemental Fig. S8A). To validate this point, we cultured the wild type, *vpt1 vpt3*, and *pht1;1* seedlings under Pi-sufficient conditions (0.3 mM) and measured Pi uptake in these plants by using the decrease of Pi in the culture solution as a proxy. Although Pi uptake efficiency was lowest in the *pht1;1* mutant, Pi uptake was also lower in *vpt1 vpt3* as compared with the wild-type seedlings (Supplemental Fig. S8B), indicating that Pi uptake efficiency of *vpt1 vpt3* is negatively affected, consistent with the reduced levels of PHT1-type

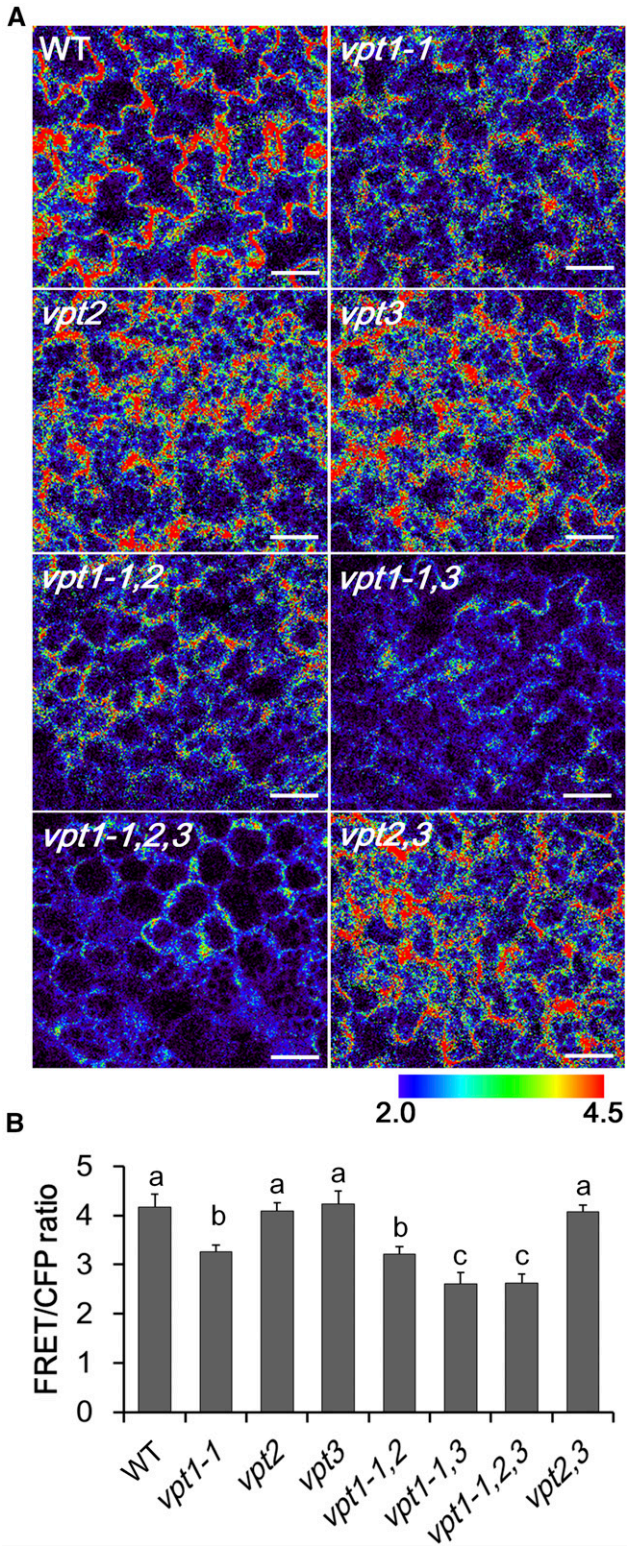

Figure 5. VPT1 and VPT3 control cytosolic Pi levels in arabidopsis mesophyll cells. A, Pi sensor (cpFLIPPi-5.3m; Mukherjee et al., 2015) was used for detecting cytosolic Pi concentration in various genotypes, including wild type; *vpt1*, *vpt2*, and *vpt3* single mutant; *vpt1 vpt2* double mutant; *vpt1 vpt3* double mutant; and *vpt1 vpt2 vpt3* triple mutant. Seedlings (10 d old) cultured in hydroponic solution with 130 μM Pi were used for fluorescence detection. Fluorescence in mesophyll cells of each genotype was detected using a confocal laser scanning microscope (Leica) with excitation wavelength at 458 nm and emission wavelength at 485/25 and 540/20 nm. Chlorophyll fluorescence could not be detected under 540/20 nm emission wavelength (Supplemental Fig. S7). The fluorescence ratio of FRET/CFP indicates cytosolic Pi concentration. At least six seedlings of each genotype were used for experiments, three biological repeats were examined, and the representative FRET ratio images were presented. WT, wild type. Bars = 50 μm. Pseudocolor was used to display the FRET/CFP ratio according to the color scale bar at bottom right in (A). B, The FRET/CFP ratio index analyses were performed using Leica software (LASAFWPF). Different letters above each bar represent statistically significant differences among genotypes ($P < 0.01$, Tukey's HSD test). Data are mean ± SD; $n = 6$ technical replicates × 3 biological replicates.

transporters in that line. Therefore, Pi uptake and vacuolar sequestration are coordinated through Pi-responsive expression of Pi uptake transporters.

The *vpt1 vpt3* Mutant Is Impaired in Reproduction

Perhaps the most striking phenotype we observed of the *vpt1 vpt3* double mutant was shortened siliques and significantly lower seed yield under sufficient Pi conditions (Fig. 6, A–C; Supplemental Fig. S9). Such phenotypes were complemented by expressing *VPT1* or *VPT3* in the double mutant background (Supplemental Fig. S10). Furthermore, this reproductive phenotype was not found in other *vpt* single or double mutants (*vpt1*, *vpt2*, *vpt3*, *vpt1 vpt2*, and *vpt2 vpt3*; Fig. 6, A–C).

We used scanning electron microscopy to explore whether the development of male and female organs was impaired in the mutants, but failed to find any morphological difference from the wild type (Fig. 6F). Hochest staining of pollen grains and in vitro pollen tube growth assays showed no significant difference between the *vpt1 vpt3* mutant and the wild type (Fig. 6, D–G).

Pi Toxicity in the Pistil Causes Reproduction Defects in *vpt1 vpt3* Mutant

At flowering stage, sufficient Pi is essential for reproduction in plants and Pi deficiency could induce late flowering and defects in seed development (Marschner, 1986; Poirier et al., 1991; Mu et al., 2008). As discussed earlier, Pi storage capacity and Pi uptake efficiency were decreased in *vpt1 vpt3*. We thus speculated that the seed set defect in *vpt1 vpt3* may be a result of impaired Pi accumulation. When we measured the Pi contents in different tissues of *vpt1 vpt3*, we found that Pi contents of *vpt1 vpt3* rosette leaves and roots were significantly lower as compared with wild-type seedlings, consistent with earlier results. To our surprise, *vpt1 vpt3* flower organs contained significantly higher Pi than the wild type (Fig. 7A). When Pi concentration in the culture solutions increased to 300 μM, the Pi

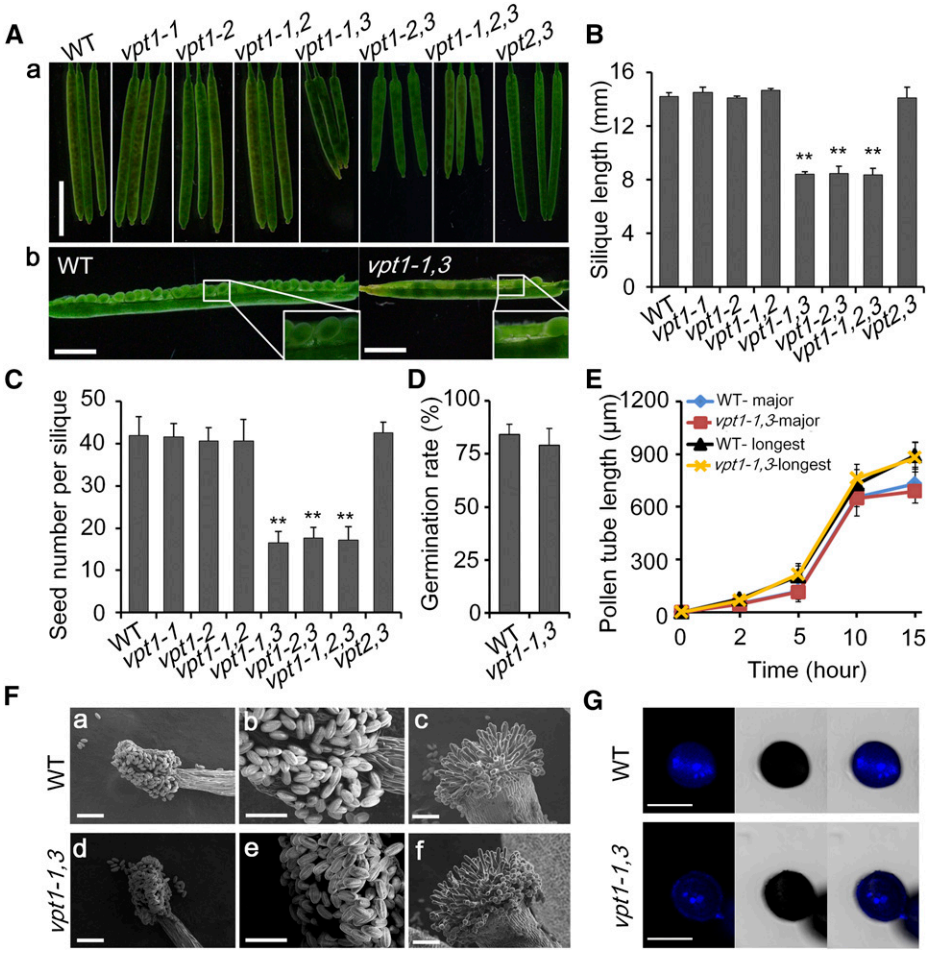

Figure 6. The *vpt1 vpt3* mutant shows defective reproduction. A, Representative siliques from wild type (WT) and various *vpt* mutants. The siliques were gathered from 5-week-old seedlings cultured in hydroponic solutions with 130 μM Pi. The white bar in (a) = 0.5 cm. Bars in (b) = 0.2 cm. B, Silique lengths of various seedlings. Data are mean ± SD; n = 8 technical replicates × 3 biological replicates. *Significant differences at $P < 0.01$ compared with wild type (Student's t test). C, Seed number in single siliques of various genotypes. Data are mean ± SD; n = 8 technical replicates × 3 biological replicates. Student's t test, **$P < 0.01$ compared with the wild type. D, Pollen germination rates of wild type and *vpt1 vpt3* in vitro. Pollen grains from 50 stage 13 to 14 flowers of each genotype were collected for measuring pollen germination rates in 4 h. A pollen grain was considered germinated when the length of the pollen tube exceeded the diameter of the pollen grain. Approximately 40 pollen grains were counted in each of 10 defined areas for each sample. Values are the mean ± SD; n = 10 technical replicates × 3 biological replicates. Student's t-test, *$P < 0.05$ compared with wild type. E, In vitro pollen tube growth of wild type and *vpt1 vpt3*. Pollen tube length was measured at 2, 5, 10, and 16 h after pollen grains were mixed with hydroponic pollen culture solution. Data are mean ± SD; n = 8 technical replicates × 3 biological replicates. F, Pollen grains and stigma in flowers of wild type and *vpt1 vpt3* under the scanning electron microscope. Bars in (a–f) = 100 μm; bars in (b and e) = 50 μm. G, Mature pollen grains of the wild type and *vpt1 vpt3* following Hochest staining. The mature pollen grains were immersed in staining solution (Hochest 33343) for 15 min and then scanned under confocal microscopy. Bars = 20 μm.

content in flower organs of *vpt1 vpt3* was about 60% higher than the wild type (Fig. 7B). Such differences also occurred, but to a much lesser extent, in the *vpt1* single mutant and *vpt1 vpt2* double mutants (Fig. 7B). Moreover, the higher the Pi concentration in the culture solution, the shorter the *vpt1 vpt3* siliques, and the fewer mature seeds produced (Fig. 7, C and D). The *vpt1 vpt3* mutants barely produced seeds under high Pi condition (300 μM). This Pi-dependent silique shortening was rescued by introducing the gene sequences of either *VPT1* or *VPT3* into the *vpt1 vpt3* double mutant (Supplemental Fig. S10). The silique length and seed set were not impaired in *vpt1* and *vpt1 vpt2* plants (Supplemental Fig. S11), likely because Pi content in *vpt1* (or *vpt1 vpt2*) flower organs was not high enough to impair reproduction. Indeed, as shown in Fig. 7B, floral Pi content of *vpt1* (or *vpt1 vpt2*) plants grown under 300 μM Pi was still lower than that of *vpt1 vpt3* grown under 130 μM Pi.

We suspected that the seed set defect in *vpt1 vpt3* mutants may result from accumulation of Pi to toxic levels in flower organs. We measured the Pi levels in

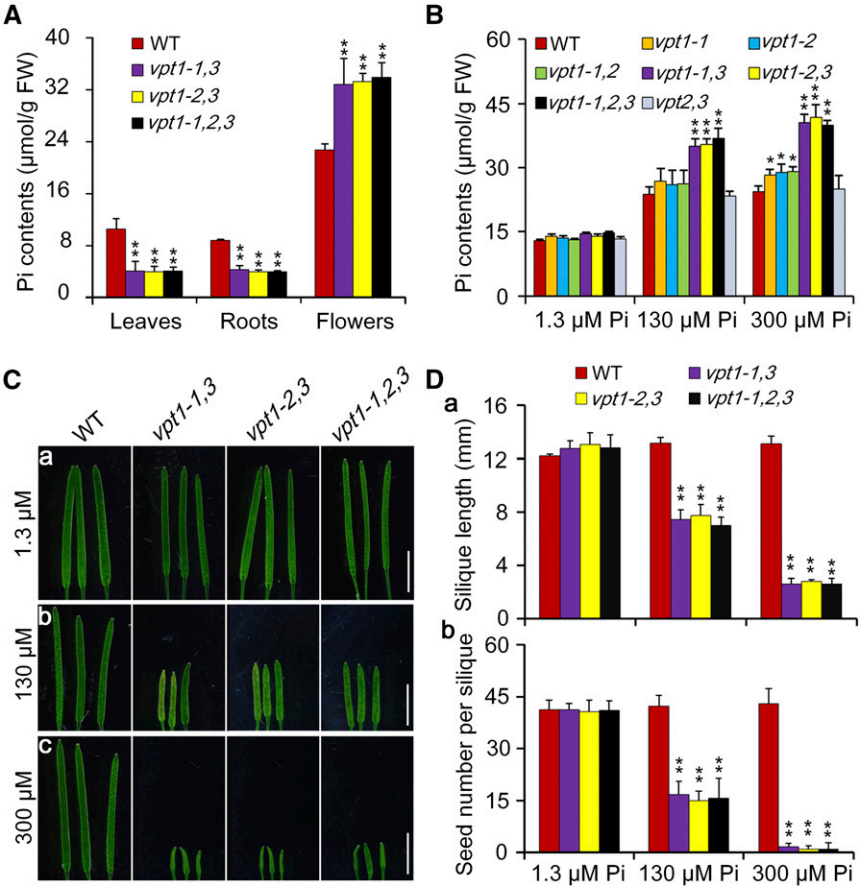

Figure 7. Pi toxicity may count for defective reproduction in the *vpt1 vpt3* mutant. A, Pi contents of rosette leaves, roots, and flower organs from wild type (WT) and mutants (*vpt1-1 vpt3*, *vpt1-2 vpt3*, and *vpt1-2 vpt2 vpt3*) cultured in 130 μM Pi. Data are mean ± SD; $n = 3$ technical replicates × 3 biological replicates. *Significant differences from wild type. Student's *t* test, $^{**}P < 0.01$. FW, fresh weight. B, Pi contents in flower organs of wild type and *vpt* mutants grown in hydroponic culture solutions with 1.3 μM, 130 μM, or 0.3 mM Pi. Data are mean ± SD; $n = 3$ technical replicates × 3 biological replicates. *Significant differences compared with wild type. Student's *t* test, $^{*}P < 0.05$, $^{**}P < 0.01$. C, Representative siliques from wild type and the *vpt1 vpt3* mutants (*vpt1-1 vpt3*, *vpt1-2 vpt3*, and *vpt1-1 vpt2 vpt3*) grown under different Pi concentration. Bars in (a–c) = 5 mm for length measurement. D, The silique length (a) and seed number per silique (b) under high Pi concentration. Data are mean ± SD; $n = 6$ technical replicates × 3 biological replicates. *Significant difference compared with wild type. Student's *t* test, $^{**}P < 0.01$.

different floral organs and found that all floral parts, including pistil, pollen, petal, and sepal, of the *vpt1 vpt3* mutant contained higher Pi than the wild type when grown under 130 μM Pi (Fig. 8A). To investigate whether female or male organs contribute to the phenotype in the mutant, we conducted reciprocal crosses between the wild type and *vpt1 vpt3* under 130 μM Pi (Fig. 8B). When the wild type was used as the female and *vpt1 vpt3* was used as a pollen donor, no defect of seed set was observed. However, when either wild type or *vpt1 vpt3* were used as the pollen donors to pollinate *vpt1 vpt3* plants, the siliques were significantly shorter and seed set was reduced as compared with the other crosses (Fig. 8B–D). When pollen tube growth on the stigma was examined by aniline blue staining, we found that pollen tube growth was normal on the wild-type stigma regardless of whether the pollen donor was wild type or *vpt1 vpt3*, whereas pollen tube elongation was inhibited when *vpt1 vpt3* was used as female receiver of wild-type or mutant pollen grains (Fig. 8, C and D). These results suggest that the seed set defect in *vpt1 vpt3* may have been caused by pollen tube growth inhibition on the mutant pistil.

We then cultured the plants under different Pi conditions and checked the effect of Pi levels on pollen tube growth. We found that both the wild type and *vpt1 vpt3* displayed normal pollen tube growth when cultured under 1.3 μM Pi (Supplemental Fig. S12A). However, when Pi concentration in the culture solution increased to 130 or 300 μM, pollen tube elongation was inhibited in the mutant but not in the wild type (Supplemental Fig. S12B). We also tested whether Pi levels directly affected pollen tube growth using the in vitro pollen tube growth assay and found that pollen germination rate was inhibited as Pi concentration increased. The pollen germination rate is only about 30% when Pi is adjusted to 3.9 mM (Supplemental Fig. S12C). In parallel, pollen tube elongation was also inhibited when 2 mM or higher Pi was added into the assay medium, and this inhibition was dose dependent (Supplemental Fig. S12E). When the germinated pollen was transferred from 0 mM Pi to 3 mM Pi solution, the elongation rate dropped from 1.25 μm/min to 0.4 μm/min (Supplemental Fig. S12D). We thus concluded that Pi over-accumulation in pistil could lead to the inhibition of pollen tube growth and reduced seed set.

Altered Long-Distance Pi Transport Contributes to Pi Toxicity in Floral Organs of *vpt1 vpt3*

The data above indicated that Pi levels in floral organs were higher in *vpt1 vpt3* than in wild-type seedlings, implying that more Pi was transported into flowers in the *vpt1 vpt3* double mutant. To validate this point, we collected and measured Pi concentrations in

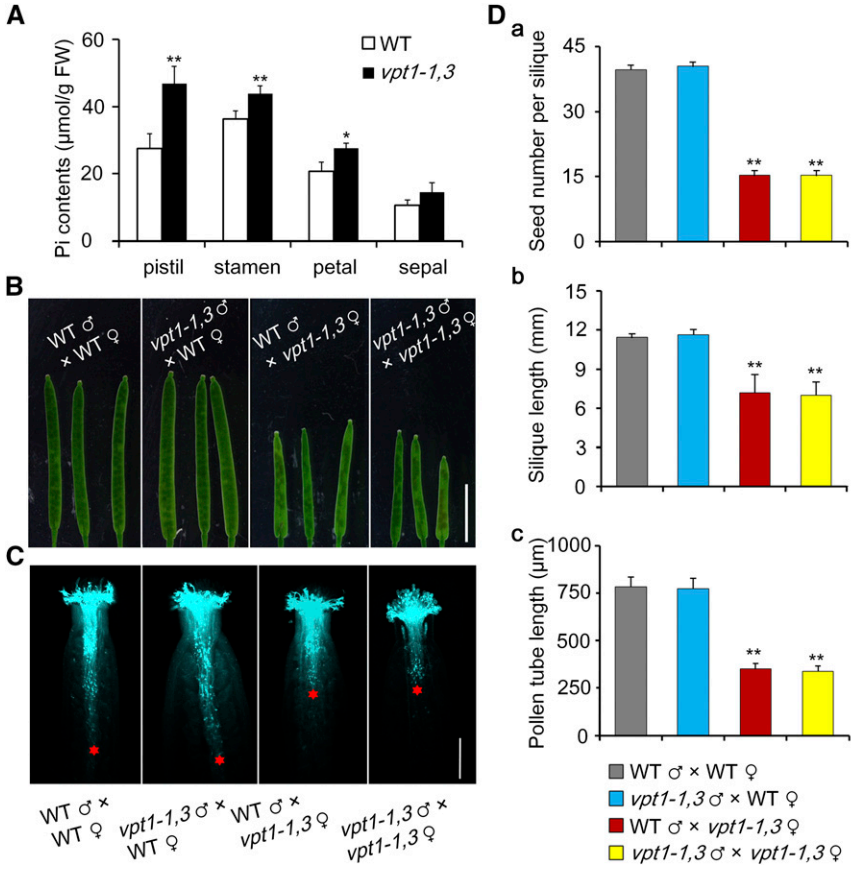

Figure 8. Excessive Pi in the pistil is responsible for impaired reproduction in *vpt1 vpt3* mutant. A, Pi contents in the floral organs of the *vpt1-1 vpt3* mutant and wild type (WT). Pistils, stamens, petals, and sepals from wild type and *vpt1-1 vpt3* plants cultured under 130 μM Pi were gathered for Pi content measurements. Data are mean ± SD; $n = 3$ technical replicates × 3 biological replicates. *Significant differences from wild type. Student's *t* test, $^*P < 0.05$, $^{**}P < 0.01$. FW, fresh weight. B, Siliques generated by crossing wild type and *vpt1 vpt3* cultured under 130 μM Pi. Bar = 5 mm. C, Aniline blue staining of pollen tubes after cross pollination. Pollen tube growth was terminated by fixation buffer 12 h after the pistils were pollinated. The samples were excited with a UV light source, and 4′,6-diamino-phenylindole emission filters were used to view the fluorescent signal from the tissue. The red stars indicate the points where most of the pollen tubes ended up in pistils. Scale bar = 250 μm for length measurement of all pollen tubes in (C). D, Quantification of seed number and silique length obtained from reciprocal crosses between wild type and *vpt1 vpt3* are presented in (a) and (b). For each cross, 10 siliques were measured. Pollen tube length (c) is quantified from repeated data in (C). Data in (D) represent the mean ± SD; $n = 10$ technical replicates × 3 biological replicates. *Significant difference as compared to wild-type seedlings (Student's *t* test, $^{**}P < 0.01$).

stem xylem sap from plants grown under various Pi levels in hydroponic cultures. The data here revealed a remarkable capacity of plants to enrich Pi from the medium. Even under the low Pi (1.3 μM) condition, Pi concentration of stem xylem sap in the wild-type plants reached about 0.2 mM, a more than 100-fold enrichment (Fig. 9A). Interestingly, we found that Pi concentration of xylem sap collected from the *vpt1 vpt3* plants was much higher as compared with the wild type. For example, when plants were grown under 130 μM Pi, xylem sap Pi was about 7.8 mM in the *vpt1 vpt3* mutant, 75% higher than that from wild type. When plants were cultured under high Pi (300 μM), Pi concentration in the stem xylem sap of *vpt1 vpt3* nearly doubled that of wild type (Fig. 9A). To ensure the measurement was done correctly, we used the *pho1* mutant as a control; the mutant should have a lower level of Pi in its xylem sap because PHO1 plays a major role in xylem loading of Pi for long-distance transport (Hamburger et al., 2002). Indeed, Pi concentration in the xylem sap of *pho1* was much lower than in the wild type (Fig. 9A). These data demonstrated that more Pi was allocated into the xylem of the floral stem in the *vpt1 vpt3* double mutant, leading to higher Pi accumulation in flowers.

If, in the *vpt1 vpt3* double mutant, more Pi was allocated into the xylem for long-distance transport, causing accumulation of toxic levels of Pi in floral organs, disruption of PHO1 in the *vpt* mutant background may remove high levels of Pi in the flowers and thus rescue the defect in reproduction in the *vpt1 vpt3* mutant. To test this hypothesis, we generated the *vpt1 vpt3 pho1* triple mutant and examined the growth and development

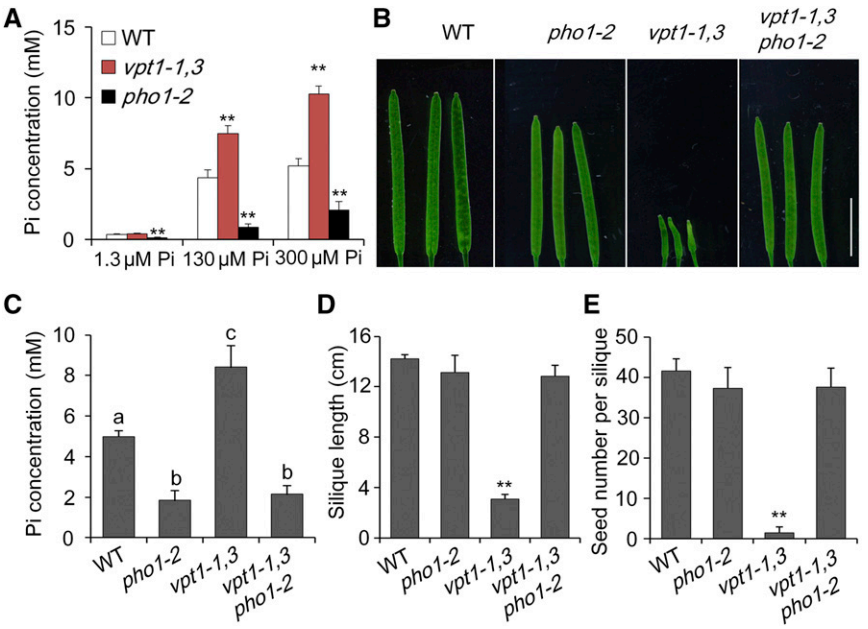

Figure 9. Altered long-distance Pi transport contributes to toxic level of Pi in flower organs of *vpt1 vpt3* double mutant. A, Stem xylem sap Pi concentration of wild type (WT), *vpt1 vpt3* and *pho1* seedlings grown under 1.3 μM, 130 μM, and 300 μM Pi. Data are mean ± SD; $n = 3$ technical replicates × 3 biological replicates. *Significant differences from wild type under the same culture conditions. Tukey's HSD test, $^{**}P < 0.01$. B, The short silique phenotype of *vpt1 vpt3* is rescued by loss-of-function of PHO1. The plants were cultured under 300 μM Pi. Bar = 5 mm. C, Stem xylem sap Pi concentration. Data are mean ± SD; $n = 3$ technical replicates × 3 biological replicates. Different letters above the each bar indicate statistically significant differences among different genotypes ($P < 0.05$, Tukey's HSD test). D, Silique length. E, Seed number per silique. Data in (D) and (E) are mean ± SD; $n = 6$ technical replicates × 3 biological replicates. *Significant differences from wild type (Student's *t* test, $^{**}P < 0.01$).

of this mutant (Fig. 9B). We conducted phenotypic assays under high Pi conditions (0.3 mM) to avoid the reproductive phenotype of *pho1* mutants due to low Pi stress (Poirier et al., 1991). Although the *vpt1 vpt3* double mutant showed severely shortened siliques as described earlier, silique length and seed numbers were similar in the *vpt1 vpt3 pho1* triple mutant and *pho1* single mutant (Fig. 9B–E). Correspondingly, Pi concentration in xylem sap of the *vpt1 vpt3 pho1* triple mutant is also similar to *pho1*, indicating that the higher level of floral Pi in the *vpt1 vpt3* mutant indeed depends on PHO1 function.

Reduced Pi Storage Capacity in *vpt1 vpt3* Leaves Impairs Systemic Pi Homeostasis

The major proportion of Pi should be allocated to leaves as they constitute the majority of the Arabidopsis plant biomass. Furthermore, the majority of Pi is stored in the vacuoles that reside in the majority of leaf cells, including epidermal and mesophyll cells (Pratt et al., 2009). At flowering stage, the xylem Pi is allocated to both leaves and flowers. When Pi sequestration capacity of leaves is defective in the *vpt1 vpt3* double mutant, a larger proportion of Pi will be transported into flowers by default, which is toxic to reproduction organs. To test this hypothesis, we performed further experiments to measure the Pi content in the xylem sap collected from the root-rosette junction and from floral stems (Fig. 10). We found that the Pi concentration of floral stem xylem sap was much higher in the *vpt1 vpt3* mutant than in the wild type as previously demonstrated (Fig. 9), but Pi concentration in the xylem sap collected from the root-rosette junction was actually slightly lower in that of the *vpt1 vpt3* double mutant compared with that in the wild-type plant, consistent with our previous data showing that Pi uptake efficiency of the *vpt1 vpt3* double mutant is down-regulated (Supplemental Fig. S8). This supports the hypothesis that mutant leaves may sequester less Pi, resulting in more Pi being transported upward to floral organs. This is also consistent with the result that *VPT1*

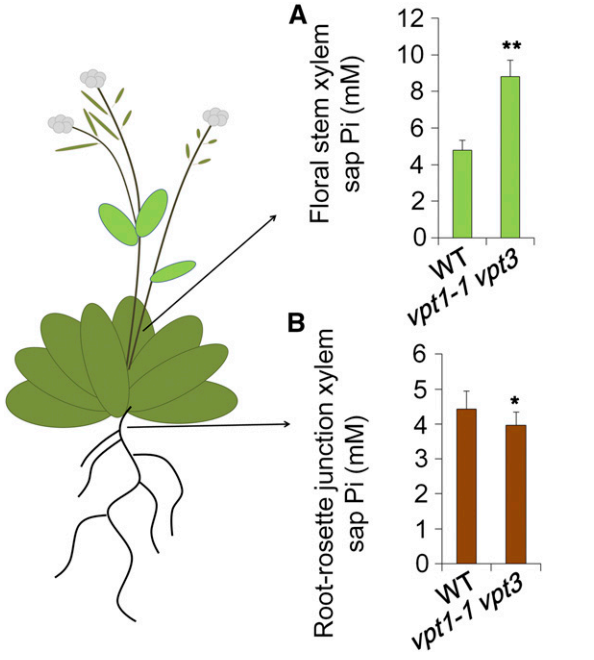

Figure 10. Pi concentrations of xylem sap collected from different parts of the plant. The xylem sap were collected from floral stem cut (A) and root-rosette junction (B). Wild-type (WT) plants and *vpt1 vpt3* double mutant were cultured under sufficient Pi condition (130 μM). Data are means ± SD; $n = 3$ technical replicates × 3 biological replicates. *Significant differences from wild type. Student's *t* test, $^{*}P < 0.05$, $^{**}P < 0.01$.

and *VPT3* are both highly expressed in leaves (Supplemental Figs. S1 and S6), which would predict a reduced vacuolar accumulation of Pi upon disruption of VPT1 and VPT3 in the mutant. To further test this hypothesis, we performed a leaf removal experiment. WT and *vpt1 vpt3* plants were both cultured under low Pi (5 μM) until flowering stage and then were transferred to high-Pi (300 μM) conditions and cultured for 3 d. The floral organs of the *vpt1 vpt3* mutant collapsed and died, whereas the flowers of wild type were not significantly affected (Fig. 11A). Stem xylem Pi content in *vpt1 vpt3* plants, as expected, was significantly higher as compared with wild type (Fig. 11B), consistent with our previous results (Fig. 9). In a parallel experiment, before the plants were transferred to high Pi solutions, all the leaves of the plants were removed (Fig. 11). At 3 d after transfer to high Pi, we observed floral death in both the wild-type (leaf removal-wild type) and the mutant plants (Fig. 11A). Additionally, leaf removal significantly increased the stem xylem Pi concentration in the wild type to 14 mM, comparable with the Pi level in the *vpt1 vpt3* plants (Fig. 11B). To link Pi levels, but not leaf removal injury, to the floral death phenotype, we also transferred some plants after leaf removal to the low-Pi condition (5 μM) and found that both wild-type and *vpt1 vpt3* flowers were not affected by leaf removal (Fig. 11A). Thus, we concluded that lack of VPT1 and VPT3 significantly reduces Pi sequestration into leaves, resulting in more Pi allocation to floral organs, leading to toxicity to reproduction under Pi sufficiency conditions.

DISCUSSION

In agriculture, low Pi availability in soil and an unsustainable P fertilizer supply represent a serious challenge to crop production. Understanding how plants adapt to low and fluctuating Pi levels in the environment may hold the key to breeding high P use efficiency in crops. Several studies suggested that although Pi status of the environment is dynamic, the cytosolic Pi (Pi_{cyt}) is kept at a relatively steady level, which is achieved mainly by cellular storage pools buffering Pi_{cyt} (Rebeille et al., 1983; Shirahama et al., 1996; Mimura, 1999; Mukherjee et al., 2015). The vacuole has been shown to provide the most important Pi storage pool in plant cells (Pratt et al., 2009). In the current study, we validated that Pi transport into the vacuole is a critical process for subcellular Pi homeostasis. The *vpt1 vpt3* mutant plants display smaller vacuolar Pi influx, resulting in higher Pi_{cyt} levels as compared with the wild-type plants under sufficient Pi conditions. Consequently, the *PSI* genes are expressed at a lower level in *vpt1 vpt3*. In the context of Pi allocation in the whole plant, reduced vacuolar sequestration leads to a larger proportion of Pi available for long-distance transport from roots to shoots, increasing Pi levels in the reproductive organs. Changes in systemic Pi allocation appear to have strong consequences in reproductive development, as we demonstrated in this study.

From flowering to seed maturation, a large amount of Pi is required for vigorous metabolism and synthesis of phytic acid ($InsP_6$), a major form of stored phosphorus in the seed (Karlen et al., 1988; Raboy, 2001; Rose et al., 2013). It is thus crucial to maintain long-distance transport from roots to the shoots during reproduction. In this context, a number of studies have focused on PHO1 family proteins that play a crucial role in long-distance Pi transport in Arabidopsis (Hamburger et al., 2002; Stefanovic et al., 2007; Liu et al., 2012; Jabnoune et al., 2013; Wege et al., 2016).

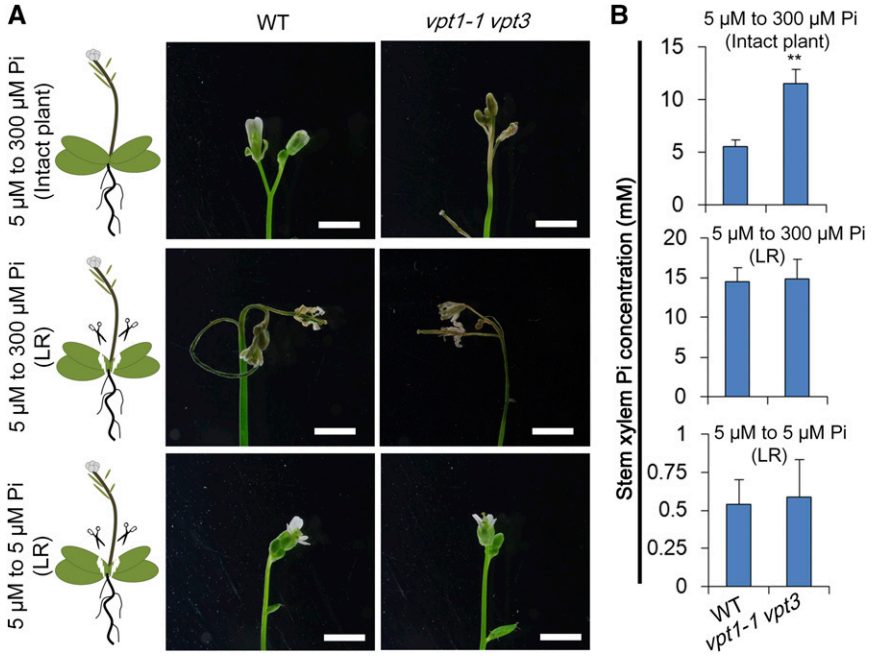

Figure 11. Leaf removal strongly enhances Pi toxicity following Pi deficiency in flower organs. A, Ten-day-old seedlings of wild type (WT) and *vpt1 vpt3* germinated on 1/2 MS plate were transferred to low Pi hydroponic solution (5 μM) and cultured for 3 weeks to flowering stage. Then the intact wild type and *vpt1 vpt3* seedlings were transferred to hydroponic solution with 300 μM Pi for 3 d. In two parallel treatments, leaves of the plants were removed (leaf removal) before transfer to 300 μM (high) or 5 μM (low) Pi-containing hydroponic solutions for 3 d. Bars = 2 mm. B, Pi concentrations in xylem sap of the plants in (A). Xylem sap was collected from floral stems of wild type and the *vpt1 vpt3* double mutant 1 d after the final transfer or leaf removal. Data are means ± SD; n = 3 technical replicates × 3 biological replicates. *Significant differences from wild type. Student's t test, $^{**}P < 0.01$.

In addition to the *OsPHO1* family members in rice, a recent report shows that node-localized SPDT (SULTR-LIKE PHOSPHORUS DISTRIBUTION TRANSPORTER) functions in maintaining the proper allocation of Pi between leaves and grains (Yamaji et al., 2017). Because phosphate is dynamically distributed based on physiological demand in different parts of a plant, regulatory mechanisms must coordinate to control long-distance transport. However, such regulatory coordination remains largely unexplored (Gu et al., 2016; Młodzińska and Zboińska, 2016; Luan et al., 2017). Here, we defined the role of VPTs in systemic Pi allocation. During the reproductive stage, root-derived Pi is transported to the aerial parts including leaves and flower organs. We show that the two genes *VPT1* and *VPT3*, both expressed in leaves, play an essential role in Pi allocation between leaves and flower organs. Loss of both VPT1 and VPT3 results in excessive Pi allocation into the floral organs rather than storage in the vacuoles of leaf cells (Fig. 12). When the external supply of Pi is sufficient, the Pi allocation to the floral organs will reach toxic levels and affect the seed set. Therefore, VPTs, through their function in vacuolar Pi sequestration, contribute to the fine-tuning of systemic Pi homeostasis during the reproductive stage, providing a new angle to view long-distance Pi transport through modulating vacuole transporters. Further, this study has made a strong connection between systemic Pi homeostasis and reproduction in plants. Clearly, either too little or too much Pi will impair reproductive development. The detailed molecular mechanisms underlying regulation of VPT-guided long-distance Pi transport require further work in the future.

Through functional analysis of the VPT family members, we found that VPT1 plays the primary role in vacuolar Pi accumulation, because the *vpt1* single mutant shows significant defects in Pi homeostasis, whereas neither the *vpt2* nor *vpt3* single mutants show any Pi-related phenotypes. Interestingly, VPT3 becomes crucial when VPT1 is disrupted, because the *vpt1 vpt3* double mutant displays more severe defects in Pi homeostasis than the *vpt1* single mutant. The role of VPT3 in vacuolar Pi sequestration was further supported by electrophysiological recording of a smaller vacuolar Pi influx current in the *vpt1 vpt3* double mutant than in the single mutants (Fig. 1). Consistent with this finding, overexpression of *VPT3* results in over-accumulation of Pi in plants (Liu et al., 2016b). The role of *VPT3* can be explained by the "compensation" effect of *VPT3* expression. When VPT1 is functional in the wild-type plants, the mRNA level of *VPT3* is kept at an extremely low level (Supplemental Figure S6C), equivalent to 4% to 5% the level of *VPT1*, which explains why disruption of VPT3 function in *vpt3* single mutant did not significantly affect Pi homeostasis. However, the expression of *VPT3* is significantly upregulated when VPT1 function is disrupted in the *vpt1* mutant. The elevated *VPT3* mRNA level in the *vpt1* mutant is equivalent to about 35% of the *VPT1* level in the wild-type plants. Such a compensation effect is pivotal for plant Pi homeostasis as reflected by several parameters.

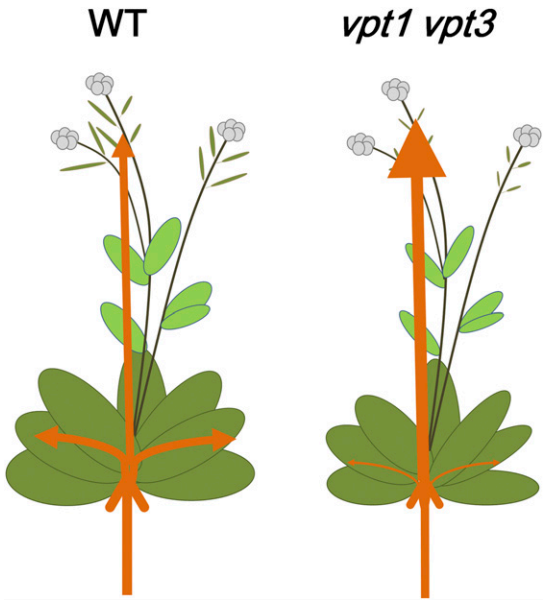

Figure 12. A schematic model showing long-distance Pi transport from roots to above-ground organs. During the reproductive stage, root-derived Pi is transported (along the arrows) to the aerial parts including leaves and flower organs. *VPT1* and *VPT3*, both expressed in leaves, play an essential role in Pi allocation between leaves and flower organs. Loss of both VPT1 and VPT3 results in excessive Pi allocation into the flower organs as a result of reduced Pi sequestration into the leaf vacuoles. When the external supply of Pi is sufficient, the Pi allocation to the flower organs can reach a toxic level and affect the seed set. WT, wild type.

First, disruption of VPT3 in the *vpt1* background (i.e. producing the *vpt1vpt3* double mutant) further compromised subcellular Pi balance as compared with the *vpt1* single mutant. The vacuolar Pi influx current densities in the *vpt1 vpt3* double mutant were further reduced as compared with the *vpt1* single mutant (Fig. 1, C and D). Correspondingly, the Pi_{cyt} level of the *vpt1 vpt3* double mutant was higher than that of the *vpt1* single mutant (Fig. 5). Second, disruption of VPT3-mediated functional compensation of *vpt1* was necessary to impair the systemic Pi homeostasis such that a toxic level of Pi was allocated to reproductive organs (Fig. 7, A and B). Such toxicity in reproduction was observed in only the *vpt1vpt3* double mutant but not in the *vpt1* single mutant, depicting the importance of VPT3-dependent compensation. The relationship between VPT1 and VPT3 might be more complicated than simple compensation at the gene expression level. Other possible mechanisms may include formation of hetero-oligomeric complexes between VPT1 and VPT3, which should be tested in future work.

MATERIALS AND METHODS

Plant Materials and Growth Conditions

Arabidopsis (*Arabidopsis thaliana*; Col-0) seedlings were used in the research for various Pi treatments. The *vpt1-1* (SAIL_96_H01), *vpt1-2* (SALK_006647), *vpt2* (SALK_009309), *vpt3* (SAIL_422_D07) T-DNA insertion mutants, and *pho1-2* were obtained from the Arabidopsis Stock Center. The hydroponic culture

solutions were prepared as previously described (Liu et al., 2015, 2016a). We used 1.3 μM NaH_2PO_4 (as the Pi resources) for low Pi treatment and 0.3 mM NaH_2PO_4 for high Pi treatment; 130 μM was used as an optimal Pi concentration.

RT-qPCR Analysis

The total RNA was extracted by using TRIzol (Invitrogen) and treated with DNaseI (Ambion) to eliminate genomic DNA. About 2 to 3 μg RNA was used for cDNA synthesis (Promega M-MLV Reverse Transcriptase). RT-qPCR was performed on a Bio-rad CFX thermocycler using Fast Start Universal SYBR Green Master Mix (Roche). The primers used for qPCR and other procedures are listed in Supplemental Table S1.

Measurements of Pi Contents

Arabidopsis seedlings grown in the hydroponic culture system were collected and washed three times in distilled water. Tissue samples of 50 mg each were used for Pi content measurement following the ascorbate-molybdate-antimony method (John, 1970).

GUS Assay

Seeds of transgenic plants harboring the GUS reporters were plated on half strength MS agar medium. The 4-d-old seedlings were transferred to hydroponic culture and grown for 14 d. Leaves of different seedlings were collected and fixed in 90% (v/v) acetone for 5 min on ice. The samples were submerged in GUS staining solution [1.9 mM X-Gluc (5-bromo-4-chloro-3-indolyl-b-D-glucuronide), 50 mM Na_2HPO_4, 50 mM NaH_2PO_4, 0.5 mM $K_4Fe(CN)_6$, 0.5 mM $K_3Fe(CN)_6$, 1% Triton X-100, 10 mM EDTA, pH 7.0] and kept under a vacuum for 15 min, flowed by incubation at 37°C for 8 h. The stained samples were incubated in 80% ethanol for pigment removal and examined under a stereoscopic microscope (Leica).

Anthocyanin Content Measurement

Anthocyanin measurement was performed as described by Teng et al. (2005). The seedlings grown under low Pi conditions were used for content assays. One absorbance unit (A530 – 0.25A657) in extraction solution represents one anthocyanin unit. Values were normalized to the fresh weight of each sample.

Root-Associated Acid Phosphatase Activity Assay

The root-associated APase activity assay was performed according to Wang et al. (2011) with some modifications. Seedlings (5 d old) germinated on 1/2 MS plates with comparable growth were transferred to solutions containing 0.1 μM Pi and cultured for another 9 d. Subsequently, seedlings were briefly rinsed in deionized water and transferred to a 1.5-mL tube containing 1.4 mL of hypotonic solution without Pi. After growing for another 3 d with gentle shaking at 23°C, the hypotonic solutions were gathered for APase activity assays. 5-Bromo-4-chloro-3-indolyl phosphate) was used as a substrate, and 600 mL of hypotonic solution containing 4 mM 5-bromo-4-chloro-3-indolyl phosphate was incubated at 37°C for 3 h. Then the reaction was terminated by adding 1 mL of 1 M HCl. After sitting at room temperature for 2 h, the samples were centrifuged for 10 min at 14,000 *g*, and the precipitates were dissolved in 1 mL of dimethyl sulfoxide. The absorbance was determined spectrophotometrically at 635 nm.

Live Imaging of the Pi Sensors in Plants

The Arabidopsis line that stably expresses the cpFLIPPi-5.3m Pi sensor protein was provided by Dr. Wayne Versaw (Mukherjee et al., 2015). We crossed various *vpt* mutants with the cpFLIPPi-5.3 sensor line and obtained homozygous mutants containing the sensor. Plants cultured under the control Pi condition (130 μM) were used to detect cytosolic Pi concentrations in the various genotypes using the previously described imaging procedure (Mukherjee et al., 2015) with a confocal laser scanning microscope (Leica TCS SP8), excitation wavelength of 458 nm and emission wavelength of 485/25 and 540/20 nm. Fluorescence from direct excitation of cpVenus was simultaneously monitored with an excitation wavelength of 500/20 nm and emission wavelength of 540/25 nm. The fluorescence ratio of FRET/CFP was used to depict relative cytosolic Pi concentration. The FRET ratios were analyzed using Leica microscope system software LASAFWPF.

Patch-Clamp Recordings on Isolated Vacuoles

Patch-clamp recordings were performed as previously described (Liu et al., 2015). The mesophyll vacuoles were isolated from 3-week-old *vpt* mutants and the wild-type seedlings grown in hydroponic culture solution with control Pi concentration. The recording was performed with the Axon Multiclamp 700B Amplifier (Molecular Devices), and the current-voltage relationships were expressed as current density (pA/pF).

Hochest Staining of Pollen

Hochest 33342 was used to stain the Arabidopsis pollen grains. Pollen grains were gathered from flowers of wild type and *vpt1 vpt3* double mutants. The pollen grains were incubated in the staining solution (5 μg/mL Hoechst 33342, 1 mM KCl, 2 mM $CaCl_2$, 1 mM $Ca(NO_3)_2$, 1 mM $MgSO_4$, pH 7.0) for 15 min in dark. Fluorescence was examined under a confocal microscope (Leica) using 405 nm excitation light. Fluorescence was detected at 430 to 550 nm.

Arabidopsis Crossing and Aniline Blue Staining

Stage 12 flowers were emasculated, and stigmas were pollinated with desired pollen grains (Smyth et al., 1990). For tracking pollen tube growth into the stigma, aniline blue staining was conducted 8 h after pollination. Pollinated pistils were fixed with 10% acetic acid in ethanol for 12 h. The samples were washed three times with distilled water, and, subsequently, pistils were incubated in 5 M NaOH overnight. Pistils were then washed three times with distilled water and stained for ~15 h with aniline blue (Fisher Scientific) [0.1% (w/v) aniline blue in 0.1 M sodium phosphate buffer, pH 7.5] in the dark. After staining, pistils are placed in a drop of 50% glycerin on a microscope slide and covered with a coverslip. Fluorescence of pollen tubes was detected using a confocal microscope (excitation: 405 nm; emission: 440 to 550 nm).

Arabidopsis Pollen Tube Growth In Vitro

Flowers from seedlings in stage 13 to 14 (Smyth et al., 1990) were collected in 2 mL Eppendorf (EP) tubes with 800 μL liquid medium [1 mM KCl, 2 mM $CaCl_2$, 1 mM $Ca(NO_3)_2$, 1 mM $MgSO_4$, 1.6 mM boric acid, 15% Suc]. The pollen grains were released into liquid medium after the EP tube was vortexed for 1 min. Supernatant was transferred to a new 1.5-mL EP tube and centrifuged at 5,000 rpm for 5 min. Pollen pellets were resuspended in 300 μL liquid medium containing various concentrations of Pi. The pollen grains were then incubated in the dark at 25°C for 8 h. For quantification of pollen tube lengths, more than 20 tubes were measured per sample under a microscope (Olympus, 10× objective). For monitoring pollen tube elongation, 2 h after germination pollen grains were transferred to different Pi-containing liquid culture medium (0 mM Pi and 3 mM Pi) and further cultured for 30 min. The growth states of pollen tubes were captured under a microscope with differential interference contrast. At least 10 tubes of each sample were detected using the microscope.

Xylem Sap Collection

Arabidopsis plants (5 weeks old) grown in hydroponic culture with control Pi concentration (130 μM) were transferred to new culture solutions containing 1.3 μM, 130 μM, or 0.3 mM Pi and cultured for 24 h. The plants were then decapitated at the bottom of the flower stem or hypocotyl by using sharp razors. The first drop of the xylem sap was discarded, and the subsequent sap was collected every 30 min for 90 min total after decapitation. High humidity (relative humidity is more than 70%) of the plant culture environment is necessary during this experiment. The xylem sap was centrifuged at 140,00 rpm to remove any debris, and 20 μL supernatant of each sample was used for Pi content measurement or stored at −80°C for later assays.

Statistical Analysis

Experiment data in this study are averages from at least three independent experiments, and the values were subjected to statistical analysis through

ANOVA followed by Student's *t* test or Tukey's honestly significant difference test (Supplemental Table S2).

Accession Numbers

Sequence data for genes and proteins presented in this article can be found in the Arabidopsis Genome Initiative of GenBank/EMBL database under the following accession numbers: *VPT1* or *PHT5;1* (AT1G63010), *VPT2* or *PHT5;2* (AT4G11810), *VPT3* or *PHT5;3* (AT4G22990), *PHT1;1* (AT5G43350), *PHT1;4* (AT2G38940), *RNS1* (AT2G02990), *IPS1* (AT3G09922), *miR399b* (AT1G63005), *PHO2* (AT2G33770) and *PHO1* (AT3G23430), *UBQ10* (AT4G05320), *ACTIN2* (AT3G18780), *γ-TIP1* (AT2G36830).

SUPPLEMENTAL DATA

The following supplemental materials are available.

Supplemental Figure S1. The expression patterns of *VPT* family members.

Supplemental Figure S2. Subcellular localization of VPT proteins (Beebo et al., 2009; Gattolin et al., 2011).

Supplemental Figure S3. Isolation of *vpt* mutant lines.

Supplemental Figure S4. *vpt1* Mutants display growth retardation.

Supplemental Figure S5. Limited Pi accumulation in the *vpt1 vpt3* double mutant was induced by loss of both VPT1 and VPT3.

Supplemental Figure S6. Expression of *VPT3* is altered in the *vpt1* mutant background.

Supplemental Figure S7. Chlorophyll dose not interfere with the FRET measurements in mesophyll cells.

Supplemental Figure S8. The Pi uptake efficiency is altered in the *vpt1 vpt3* mutant.

Supplemental Figure S9. Phenotype of various double and triple mutants cultured in soil.

Supplemental Figure S10. Impaired seed set in *vpt1 vpt3* mutant is compensated by expressing genome sequence of *VPT1* or *VPT3*.

Supplemental Figure S11. Defective reproductive development in *vpt1 vpt3* double mutant depends on Pi status.

Supplemental Figure S12. High level of Pi inhibits pollen tube growth both in vivo and in vitro.

Supplemental Table S1. A second reference gene (*Actin2*) was used for validation of the qPCR data in Supplemental Figure S5, A–C.

Supplemental Table S2. Primers used in this study.

Supplemental Table S3. Statistical analysis table.

ACKNOWLEDGMENTS

We thank Dr. Shiyou Lv for providing the *Arabidopsis pho2-1* mutant seeds and Dr. Wayne Versaw for providing the Pi biosensor (cpFLIPPi-5.3m) line. We thank Jiangsu Collaborative Innovation Center for Modern Crop Production for technical support.

Received November 13, 2018; accepted December 5, 2018; published December 14, 2018.

LITERATURE CITED

Ai P, Sun S, Zhao J, Fan X, Xin W, Guo Q, Yu L, Shen Q, Wu P, Miller AJ, et al (2009) Two rice phosphate transporters, OsPht1;2 and OsPht1;6, have different functions and kinetic properties in uptake and translocation. Plant J **57:** 798–809

Arpat AB, Magliano P, Wege S, Rouached H, Stefanovic A, Poirier Y (2012) Functional expression of PHO1 to the Golgi and trans-Golgi network and its role in export of inorganic phosphate. Plant J **71:** 479–491

Aung K, Lin SI, Wu CC, Huang YT, Su CL, Chiou TJ (2006) *pho2*, a phosphate overaccumulator, is caused by a nonsense mutation in a microRNA399 target gene. Plant Physiol **141:** 1000–1011

Beebo A, Thomas D, Der C, Sanchez L, Leborgne-Castel N, Marty F, Schoefs B, Bouhidel K (2009) Life with and without AtTIP1;1, an Arabidopsis aquaporin preferentially localized in the apposing tonoplasts of adjacent vacuoles. Plant Mol Biol **70:** 193–209

Gattolin S, Sorieul M, Frigerio L (2011) Mapping of tonoplast intrinsic proteins in maturing and germinating Arabidopsis seeds reveals dual localization of embryonic TIPs to the tonoplast and plasma membrane. Mol Plant **4:** 180–189

Gu M, Chen A, Sun S, Xu G (2016) Complex regulation of plant phosphate transporters and the gap between molecular mechanisms and practical application: What is missing? Mol Plant **9:** 396–416

Hamburger D, Rezzonico E, MacDonald-Comber Petétot J, Somerville C, Poirier Y, Borst JW, Hamburger D, Rezzonico E, MacDonald-Comber Petetot J, Somerville C, et al (2002) Identification and characterization of the *Arabidopsis* PHO1 gene involved in phosphate loading to the xylem. Plant Cell **14:** 889–902

Huang TK, Han CL, Lin SI, Chen YJ, Tsai YC, Chen YR, Chen JW, Lin WY, Chen PM, Liu TY, et al (2013) Identification of downstream components of ubiquitin-conjugating enzyme PHOSPHATE2 by quantitative membrane proteomics in Arabidopsis roots. Plant Cell **25:** 4044–4060

Jabnoune M, Secco D, Lecampion C, Robaglia C, Shu Q, Poirier Y (2013) A rice cis-natural antisense RNA acts as a translational enhancer for its cognate mRNA and contributes to phosphate homeostasis and plant fitness. Plant Cell **25:** 4166–4182

Jia H, Ren H, Gu M, Zhao J, Sun S, Zhang X, Chen J, Wu P, Xu G (2011) The phosphate transporter gene OsPht1;8 is involved in phosphate homeostasis in rice. Plant Physiol **156:** 1164–1175

John MK (1970) Colorimetric determination of phosphorus in soil and plant materials with ascorbic acid. Soil Sci **109:** 214–220

Karlen DL, Flannery RA, Sadler EJ (1988) Aerial accumulation and partitioning of nutrients by corn. Agron J **80:** 232–242

Kim W, Ahn HJ, Chiou TJ, Ahn JH (2011) The role of the miR399-PHO2 module in the regulation of flowering time in response to different ambient temperatures in *Arabidopsis* thaliana. Mol Cells **32:** 83–88

Li S, Ying Y, Secco D, Wang C, Narsai R, Whelan J, Shou H (2017) Molecular interaction between PHO2 and GIGANTEA reveals a new crosstalk between flowering time and phosphate homeostasis in Oryza sativa. Plant Cell Environ **40:** 1487–1499

Liu J, Yang L, Luan M, Wang Y, Zhang C, Zhang B, Shi J, Zhao FG, Lan W, Luan S (2015) A vacuolar phosphate transporter essential for phosphate homeostasis in *Arabidopsis*. Proc Natl Acad Sci USA **112:** E6571–E6578

Liu J, Fu S, Yang L, Luan M, Zhao F, Luan S, Lan W (2016a) Vacuolar SPX-MFS transporters are essential for phosphate adaptation in plants. Plant Signal Behav **11:** e1213474

Liu TY, Huang TK, Tseng CY, Lai YS, Lin SI, Lin WY, Chen JW, Chiou TJ (2012) PHO2-dependent degradation of PHO1 modulates phosphate homeostasis in Arabidopsis. Plant Cell **24:** 2168–2183

Liu TY, Huang TK, Yang SY, Hong YT, Huang SM, Wang FN, Chiang SF, Tsai SY, Lu WC, Chiou TJ (2016b) Identification of plant vacuolar transporters mediating phosphate storage. Nat Commun **7:** 11095

Luan M, Tang RJ, Tang Y, Tian W, Hou C, Zhao F, Lan W, Luan S (2017) Transport and homeostasis of potassium and phosphate: Limiting factors for sustainable crop production. J Exp Bot **68:** 3091–3105

Marschner H (1986) Functions of Mineral Nutrients: Macronutrients. Mineral Nutrition of Higher Plant. Academic Press, London, pp 226–235

Mimura T (1999) Regulation of phosphate transport and homeostasis in plant cells. Int Rev Cytol **191:** 149–200

Misson J, Thibaud MC, Bechtold N, Raghothama K, Nussaume L (2004) Transcriptional regulation and functional properties of *Arabidopsis* Pht1;4, a high affinity transporter contributing greatly to phosphate uptake in phosphate deprived plants. Plant Mol Biol **55:** 727–741

Młodzińska E, Zboińska M (2016) Phosphate uptake and allocation—a closer look at *Arabidopsis thaliana L.* and *Oryza sativa L.* Front Plant Sci **7:** 1198

Mu P, Huang C, Li J-X, Liu L-F, Li Z-C (2008) Yield trait variation and QTL mapping in a DH population of rice under phosphorus deficiency. Zuo Wu Xue Bao **34:** 1137–1142

Mukherjee P, Banerjee S, Wheeler A, Ratliff LA, Irigoyen S, Garcia LR, Lockless SW, Versaw WK (2015) Live imaging of inorganic phosphate in plants with cellular and subcellular resolution. Plant Physiol **167:** 628–638

Poirier Y, Thoma S, Somerville C, Schiefelbein J (1991) Mutant of *Arabidopsis* deficient in xylem loading of phosphate. Plant Physiol **97:** 1087–1093

Pratt J, Boisson AM, Gout E, Bligny R, Douce R, Aubert S (2009) Phosphate (Pi) starvation effect on the cytosolic Pi concentration and Pi exchanges across the tonoplast in plant cells: An in *vivo* 31P-nuclear magnetic resonance study using methylphosphonate as a Pi analog. Plant Physiol **151:** 1646–1657

Raboy V (2001) Seeds for a better future: 'Low phytate' grains help to overcome malnutrition and reduce pollution. Trends Plant Sci **6:** 458–462

Rebeille F, Bligny R, Martin JB, Douce R (1983) Relationship between the cytoplasm and the vacuole phosphate pool in *Acer pseudoplatanus* cells. Arch Biochem Biophys **225:** 143–148

Rose TJ, Liu L, Wissuwa M (2013) Improving phosphorus efficiency in cereal crops: Is breeding for reduced grain phosphorus concentration part of the solution? Front Plant Sci **4:** 444

Shin H, Shin HS, Dewbre GR, Harrison MJ (2004) Phosphate transport in *Arabidopsis*: Pht1;1 and Pht1;4 play a major role in phosphate acquisition from both low- and high-phosphate environments. Plant J **39:** 629–642

Shirahama K, Yazaki Y, Sakano K, Wada Y, Ohsumi Y (1996) Vacuolar function in the phosphate homeostasis of the yeast *Saccharomyces cerevisiae*. Plant Cell Physiol **37:** 1090–1093

Smyth DR, Bowman JL, Meyerowitz EM (1990) Early flower development in *Arabidopsis*. Plant Cell **2:** 755–767

Stefanovic A, Ribot C, Rouached H, Wang Y, Chong J, Belbahri L, Delessert S, Poirier Y (2007) Members of the PHO1 gene family show limited functional redundancy in phosphate transfer to the shoot, and are regulated by phosphate deficiency via distinct pathways. Plant J **50:** 982–994

Teng S, Keurentjes J, Bentsink L, Koornneef M, Smeekens S (2005) Sucrose-specific induction of anthocyanin biosynthesis in Arabidopsis requires the MYB75/PAP1 gene. Plant Physiol **139:** 1840–1852

Vance CP, Uhde-Stone C, Allan DL (2003) Phosphorus acquisition and use: Critical adaptations by plants for securing a nonrenewable resource. New Phytol **157:** 423–447

Van Kauwenbergh SJ, Stewart M, Mikkelsen R (2013) World reserves of phosphate rock—a dynamic and unfolding story. Better Crops **97:** 18–20

Wang L, Li Z, Qian W, Guo W, Gao X, Huang L, Wang H, Zhu H, Wu JW, Wang D, et al (2011) The Arabidopsis purple acid phosphatase AtPAP10 is predominantly associated with the root surface and plays an important role in plant tolerance to phosphate limitation. Plant Physiol **157:** 1283–1299

Wang X, Wang Y, Piñeros MA, Wang Z, Wang W, Li C, Wu Z, Kochian LV, Wu P (2014) Phosphate transporters OsPHT1;9 and OsPHT1;10 are involved in phosphate uptake in rice. Plant Cell Environ **37:** 1159–1170

Wege S, Khan GA, Jung JY, Vogiatzaki E, Pradervand S, Aller I, Meyer AJ, Poirier Y (2016) The EXS domain of PHO1 participates in the response of shoots to phosphate deficiency via a root-to-shoot signal. Plant Physiol **170:** 385–400

Wild R, Gerasimaite R, Jung JY, Truffault V, Pavlovic I, Schmidt A, Saiardi A, Jessen HJ, Poirier Y, Hothorn M, et al (2016) Control of eukaryotic phosphate homeostasis by inositol polyphosphate sensor domains. Science **352:** 986–990

Withers PJ, Sylvester-Bradley R, Jones DL, Healey JR, Talboys PJ (2014) Feed the crop not the soil: Rethinking phosphorus management in the food chain. Environ Sci Technol **48:** 6523–6530

Wudick MM, Portes MT, Michard E, Rosas-Santiago P, Lizzio MA, Nunes CO, Campos C, Santa Cruz Damineli D, Carvalho JC, Lima PT, et al (2018) CORNICHON sorting and regulation of GLR channels underlie pollen tube Ca^{2+} homeostasis. Science **360:** 533–536

Yamaji N, Takemoto Y, Miyaji T, Mitani-Ueno N, Yoshida KT, Ma JF (2017) Reducing phosphorus accumulation in rice grains with an impaired transporter in the node. Nature **541:** 92–95